Toward Gamma Ray Immune Fibre-Optic Phosphor Thermometry for Nuclear Decommissioning

Nicolò Pisani[1] · **Eric Numkam Fokoua[1]** · **Ian A. K. Davidson[1]** ·
Francesco Poletti[1] · **Radan Slavík[1]** · **Dave Lowe[2]** · **Graham Machin[2]** ·
Gavin Sutton[2]

Abstract

Temperature measurement of stored nuclear waste is important for long-term monitoring. Conventional sensors can degrade in ionizing radiation from induced transmutations and their frequent replacement is inconvenient. A thermometer based on suitable phosphors can overcome some problems, but the optical signal needs to be transmitted through an optical fibre and processed remotely away from the dangerous area. This requires that the optical fibre itself be suitably resistant to radiation-induced damage. Here, we report transmission measurements through a type of hollow-core fibre based on anti-resonance and with transmission windows at wavelengths suitable for use with the thermographic phosphor magnesium fluorogermanate whilst subjected to gamma radiation. Its performance is compared to commercially available standard fibres (single mode and radiation hard fibres) at dose rates equivalent to decades of use in a storage facility. Transmission was unchanged for the anti-resonant fibre at the phosphor emission wavelength and it was successfully incorporated into a fibre thermometer that worked from 20 °C to 200 °C. Performance at the phosphor excitation wavelength needs to be improved by modification to the hollow-core fibre design, but we show that a hybrid of single mode and anti-resonant fibres can already be made into a thermometer with suitable gamma immunity.

Keywords Anti-resonance · Hollow-core fibre · Nuclear waste storage · Phosphor ratio thermometry · Radiation-induced damage

---

✉ Nicolò Pisani
  N.Pisani@soton.ac.uk

Extended author information available on the last page of the article

1 Introduction

Many countries which use atomic energy for electricity production are now decommissioning their first- and second-generation nuclear facilities [1]. There is a need to safely treat and store the radioactive materials. Reliable temperature measurement is necessary for the purposes of health monitoring and corrosion modelling but must be operated remotely. However, commonly used temperature sensors (such as thermocouples, resistance- and infrared-thermometers) present several difficulties when applied to nuclear decommissioning contexts which are not only difficult to access but can also induce physical and chemical changes and hazards. Surface temperature measurements are particularly difficult. Contact sensors can themselves be damaged by transmutation, and changes in the object being measured such as oxidation, corrosion, and densification can unpredictably alter, for example, heat-flux rate, contact thermal resistance and thermal radiance. Errors up to 20 °C even at a relatively low temperature of 80 °C have been reported for both thermocouples and radiation thermometers [2] This makes it difficult for those monitoring the waste to tell what might be a problem that needs addressing rather than what is a problem with thermometry.

Phosphors have the possibility to make standoff measurements: once a phosphor coat has been applied to a substrate whose temperature is ought to be measured, it can be illuminated and the resulting emission monitored from a distance. They are, in a sense, a semi-non-contact method. One phosphor coating, manganese activated magnesium fluorogermanate (Mg4GeO5, 5F:Mn—henceforth MFG) mixed with a silicone-based binder, has been shown to be unchanged by high exposure to ionising radiation [3]. However, there are times when significant standoff distances may be required or direct line-of-sight may not be possible. Fibre optics could be used to increase standoff distance, allow indirect access or could be fabricated into a contact sensor somewhat equivalent to a thermocouple. For this to work, the fibre used to illuminate the phosphor at the excitation wavelength and receive at the emission wavelength needs to have high transmission at those wavelengths throughout its lifetime. Conventional silica-based optical fibres are liable to darken and degrade with exposure to gamma radiation [4], but one possibility is to use a class of novel optical fibres which guide light in a hollow, air-filled or indeed vacuum-filled core. Here, the fibre structure is carefully designed to make low loss confinement and guidance within a central void region possible. In such fibres, very little light is transmitted in the solid material of the fibre so the effect of radiation-induced damage can be orders of magnitude smaller than in standard fibres. Although such fibres have been predominantly researched for optimum operation at telecommunication wavelengths where they offer extremely compelling advantages over standard fibres, they have also shown remarkable performance at other wavelengths and it is believed this sustained progress will soon make them outperform all other fibre types at all spectral wavelengths [5–10]. So far however, this class of fibre has never been used for phosphor thermometry, and its suitability for operation in such an application and under gamma irradiation has not yet been explored.

There are a number of steps involved in making such a fully fledged hollow-core fibre-based thermometer:

- assessing the feasibility of using novel hollow-core fibres;
- assessing the fibre's ability to collect the emission from the phosphor;
- optimising design of the fibre and its properties;
- designing means of reliably attaching the phosphor to the fibre and accurate calibration of the device.

In this paper we focus on the first two points. We investigate the effect of gamma radiation on a hollow-core fibre sample that transmits light at wavelengths suitable to MFG (excitation in UV-blue and emission in visible red). Our results show that the fibre's performance is virtually immune to the ionising radiation at the phosphor emission wavelength of 635 nm. The apparent impairment in its transmission at the MFG excitation wavelength of 450 nm, used in this work, originates from other effects in the fibre unrelated to radiation. Using a commercially available standard fibre showing good radiation hardness at the excitation wavelength, we demonstrate the hollow-core fibre's ability to collect the light emitted by the phosphor by building, for the first time, a hybrid MFG thermometer using the solid fibre for the excitation and the hollow-core fibre for collection. The phosphor thermometer operates using the intensity ratio technique and is shown to reliably measure temperatures from 20 °C to 200 °C.

2 Anti-resonant Hollow-Core Fibres

Most of today's optical fibres guide light in a solid glass core by means of total internal reflection which requires the fibre's core material to have a higher refractive index than the surrounding cladding. However, the past two decades have seen the emergence of hollow-core fibres in which light propagates through an empty core with a refractive index close to 1, and which thus rely on different guiding mechanisms [11, 12] . The hollow-core fibres used in this work guide via a mechanism known as 'antiresonance'. Its principle can be explained using the so-called ARROW (Anti-resonant Reflecting Optical Waveguide) model [13], which is schematically illustrated in Fig. 1a. In our illustration, light propagates in the void region between two thin slabs of glass that have refractive index n and thickness d. Each glass slab can be regarded as a Fabry–Pérot etalon. When the wavelength of the propagating light is resonant in these etalons, it will pass through, escaping from the central region. However, for wavelengths between these resonances, most of the light will be reflected, remaining trapped between the two glass slabs. This 'out of resonance', or spectral regions at which little light escape through the slabs give the name to this guiding mechanism: antiresonance.

Through simple and straightforward derivations, it can be shown that for near grazing incidence on the slabs, the resonant wavelengths λ_m are given by [14]:
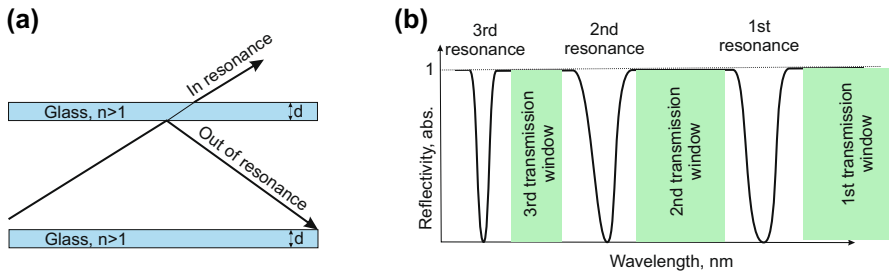
Fig. 1 (a) ARROW model of an anti-resonant waveguide. Glass slabs serve as Fabry–Perot etalons. Light incident on the glass slab is transmitted when resonant in the Fabry–Perot etalon (escaping) or strongly reflected when out of the resonance. (b) First three resonances and associated anti-resonance windows, where most of the light is trapped between the glass slabs

$$\lambda_m = \frac{2d}{m}\sqrt{n^2 - 1}, \quad m = 1, 2 \ldots, \tag{1}$$

where the integer m is the resonance order, see Fig. 1a. Between the resonances, most of the light is reflected from the glass slabs, effectively trapping it in between the two slabs and thus forming transmission windows, as schematically shown in Fig. 1b.

After more than a decade of research [15], it has been found that to best exploit this concept of anti-resonance in optical fibre geometry, the thin glass slabs are replaced by a number of non-contacting thin glass tubes arranged around a central void region which is the core and attached to a silica jacket, as shown in Fig. 2a. The fundamental core-guided mode of such a fibre is shown in Fig. 2b and resembles the typical Gaussian profile of standard optical fibres, albeit with an azimuthal symmetry defined by the number of tubes used for the cladding. The particularity of
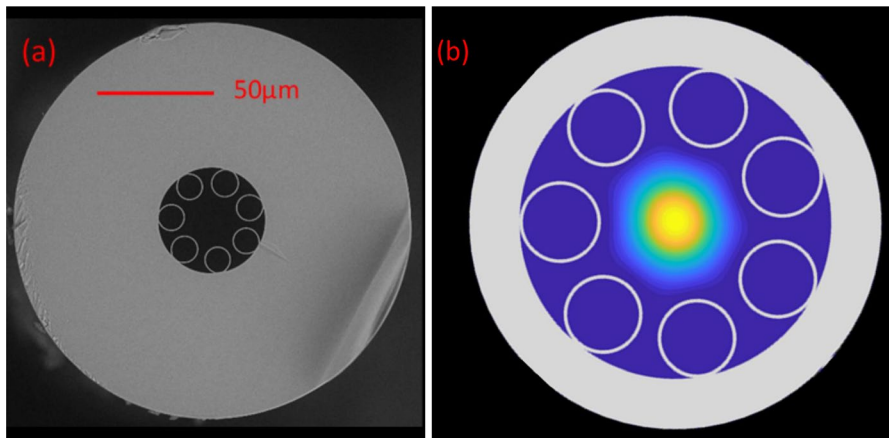

Fig. 2 Example of anti-resonant hollow-core fibre (a) SEM image of fibre used in this work and (b) calculated fundamental mode field profile, showing close resemblance to a Gaussian mode

such a hollow-core optical fibre is that most of the optical mode's energy propagates through the central hole with a vanishingly small amount (10 s of ppm) propagating in the glass material. This ensures that the loss of the core-guided modes is significantly less sensitive to changes in the attenuation of the glass material, unlike in traditional glass-core fibres where the mode field would "see" all such changes. As a result, we expect hollow-core fibres to offer significantly robust resistance to the detrimental effects of ionizing radiation which in standard fibres lead to radiation-induced attenuation. This robustness is further enhanced by the fact that hollow-core fibres are typically made using pure silica whose response to ionizing radiation is smaller than that of germanium-doped silica often found in the core of solid-core fibres [16].

3 Phosphor Thermometry

The use of phosphor powders for thermometry is a well-established technique [17]. Thermographic phosphors that are excited by an external light source at one wavelength emit at a different wavelength in a way that is temperature dependent. Often powders are seeded into liquid and used to combine temperature and velocity maps [18], but they can also be mixed with a binder and applied to an object to measure surface temperature. Previous work has shown that there are MFG-binder combinations that are suitable for use in nuclear decommissioning and waste storage conditions [3] and that this phosphor coating can be used as an emissivity-free alternative to thermal imaging [2]. Phosphors have competing decay mechanisms—radiative by an electron change of energy level (photon) or thermal by lattice vibration (phonon). As temperature increases the phonon mechanism increases and the number of electrons available to contribute photons decreases. Above a certain temperature, phonon relaxation will dominate over radiative relaxation and there will be no more emission (the phosphor is quenched). Phosphors suitable for thermographic use have a monotonic temperature dependence beyond a simple decrease in intensity, and temperature can be determined either from a change of time constant of the phosphor decay [19] or from changes in the emitted spectrum [20].

4 Radiation Hardness Measurements

To investigate the suitability of hollow-core anti-resonant fibres for phosphor-based thermometry in ionizing radiation environments, we first characterize its transmission performance when exposed to ionizing radiation from a Cobalt 60 source. The sample used here was engineered at the University of Southampton and a scanning electron micrograph of its cross section is shown in Fig. 2a. Further details on this fibre are given below. For comparison and benchmark purposes, we simultaneously perform similar measurements on two additional conventional fibre samples. The first is a commercially available radiation hard single mode solid-core fibre (RHF) from iXblue. It is designed for reduced radiation-induced attenuation in the 1300 nm to 1600 nm spectral range and although these wavelengths do not align with the

excitation or emission of the MFG phosphor, there are to the best of our knowledge, no commercially available 'radiation-hard' fibres designed for shorter wavelengths. The second is a commercially available single mode fibre with a pure silica core and a cladding doped to reduce its refractive index from Thorlabs. We chose this fibre because the literature suggests that pure silica is generally less sensitive to radiation than the doped silica often used in fibre cores [4]. Table 1 below summarises the key parameters of the three fibre samples we tested.

Figure 2a is a scanning electron microscope image of the cross-section of the anti-resonant hollow-core fibre we fabricated in-house. It has a core diameter of 22.4 μm and we have calculated the mode field diameter of its fundamental mode to be 15.7 μm. The average thickness of the cladding tubes is 507 nm, which from Fig. 1 means this fibre guides 450 nm light in the 3rd anti-resonance window and 600 nm to 700 nm light in the 2nd anti-resonance window.

The confinement loss of the fibre measured via cutback is shown in Fig. 3a along with numerically simulated loss values, showing in this instance a good agreement to within a factor of two. Note that the measured low loss region of the third anti-resonant window is much narrower than the simulated one. This is due to micro-bend-induced loss mechanisms that are not included in the simulation model. In Fig. 3b we show the calculated radiation-induced attenuation (RIA) in this fibre, displaying thanks to extremely low overlap of the guided mode and the glass material a remarkable four to five orders of magnitude reduction over the RIA in pure silica (from [21]).

The experimental set-up used for testing the sensitivity to radiation is shown in Fig. 4. All components were fibre-pigtailed, making the assembly very straightforward (requiring only fibre splicing) and alignment-free once assembled. Fibre-coupled laser diodes (LDs) emitting at 450 nm and 635 nm were first combined using a wavelength combiner (commonly referred to as a wavelength division multiplexed (WDM) combiner). Its output was spliced with the fibres under test (FUTs) that were 70 nm long (77 m for the hollow-core fibre). For each sample, 50 m was wound on a bobbin, the rest of the length was used to deliver light to/from the irradiation zone to the rest of the set-up placed in the adjacent control room. At their output, light was then sent to a photo-detector (PD). A slightly different approach was chosen for the SMF, which is significantly cheaper than the wavelength combiner. Here, two samples were used, each transmitting only one wavelength. The PDs and LDs were controlled through a computer, which used a custom routine to switch on blue LDs for 10 s, collect transmission data and then switch on the red LDs, collecting

Table 1 Material constituents of the fibre samples used in the experiments

Fibre code	Label	Core	Cladding
IXF-SM-1550 125-014HT[1]	RHF	Doped silica	F-doped silica
Hollow-core fibre	HCF	Air	Pure silica
S405-XP[2]	SMF	Pure silica	F-doped silica

[1]https://photonics.ixblue.com/product/fibres/ixf-sm-1550-125-014-ht
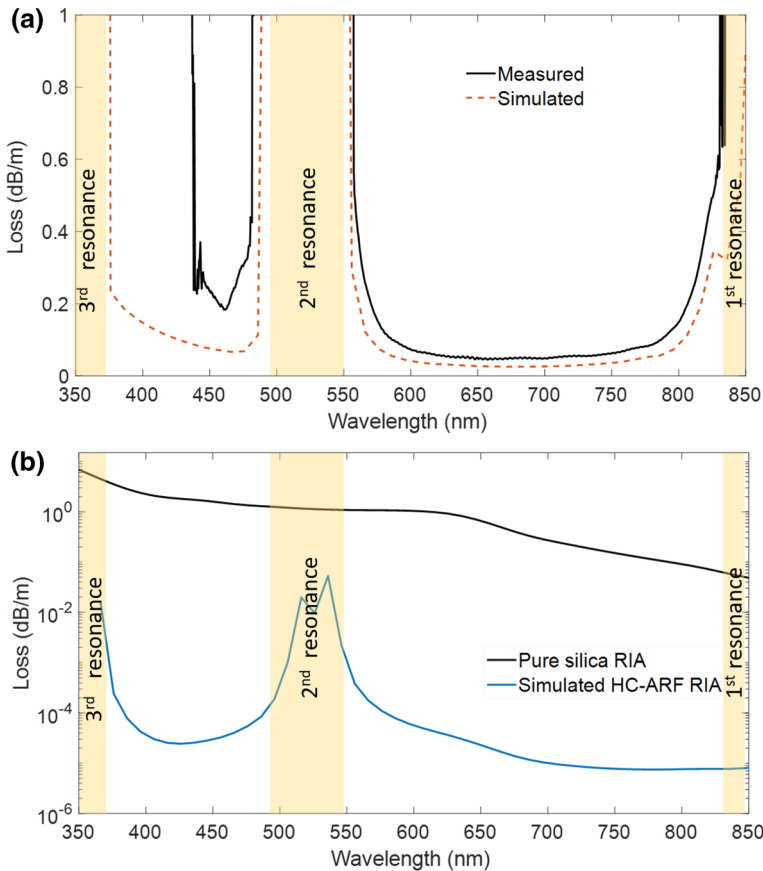[2]https://www.thorlabs.com/thorproduct.cfm?partnumber=S405-XP

Fig. 3 Transmission losses of the manufactured hollow-core anti-resonant fibre, (a) comparison between confinement loss measured via cutback to finite element simulations and (b) simulated radiation-induced loss penalty (blue curve) compared to the radiation-induced loss in pure silica core single mode fibre (data from [21])

transmitted powers at that wavelength for another 10 s, and then repeating the process. We wound all four FUTs on the same bobbin and the assembly was irradiated by a Cobalt 60 source at the National Physical Laboratory. As each FUT is at slightly different vertical position and distance from the irradiation source, the dose each receives is different. Prior to our experiments, the dose at the location of each fibre sample was measured and is summarised in Table 2.

We acquired transmission data through the four fibre samples for a duration of 90 h in total. For the first 18 h, the irradiation source was off, allowing us to collect baseline data for comparison and calibration. The Cobalt 60 source was then switched on for the following 72 h. This duration was chosen to allow each of the fibres to receive at least a few kGy total dose, as summarised in Table 2. These levels of irradiation were targeted as these are typical of the environments where our thermometers might be deployed, notably in waste monitoring at nuclear
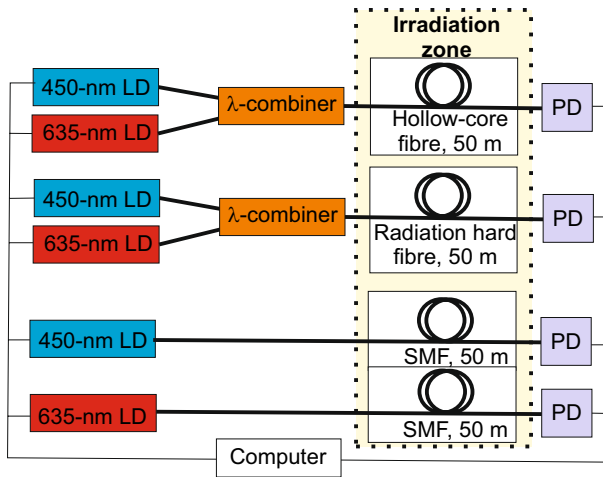
Fig. 4 Schematic of the self-built experimental set-up utilized in this work to measure radiation-induced attenuation in FUTs

Table 2 Flux and fluence values of gamma field during radiation hardness test with samples relative distances from the source

Fibre sample	Distance from source (cm)	Dose rate (Gy h^{-1})	Total absorbed dose (kGy)
RHF	90	51.0 ± 2.5	3.7 ± 0.2
SMF-2	85	56.9 ± 2.8	4.1 ± 0.2
SMF-1	80	68.1 ± 3.4	4.9 ± 0.2
HCF	74	75.2 ± 3.8	5.4 ± 0.3

decommissioning sites where they may need to be in use for up to 25 years (see [22]).

5 Results—Radiation-Induced Attenuation

Figures 5, 6 and 7 show the recorded transmission through the fibre samples at both laser wavelengths as they were subjected to irradiation. Starting with the RHF, for which the transmission is shown in Fig. 5, both blue and red signals propagating through it decay almost instantly to the noise floor after the irradiation source is turned on. We speculate that this highly unexpected behaviour may be due to the fact that in designing the fibre for radiation hard operation in the 1300 nm to 1600 nm band, dopants might have been used in the glass which inadvertently increased its radiation-induced attenuation at short wavelengths. Though full details about the dopants used and the composition of the glass are kept confidential by the manufacturer, one plausible scenario may be that of dopant-induced self-trapped holes (or electrons), i.e. ripped-off charge carriers
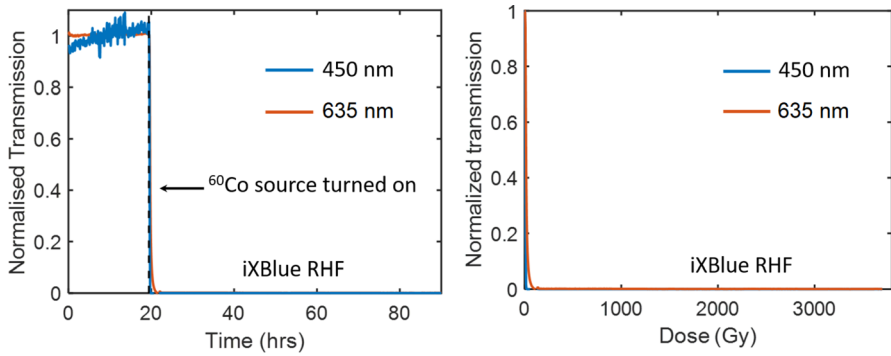
Fig. 5 Normalized transmitted optical power for MFG phosphors excitation/emission wavelengths through the radiation hard fibre (RHF) as a function of time (left) and received dose (right)
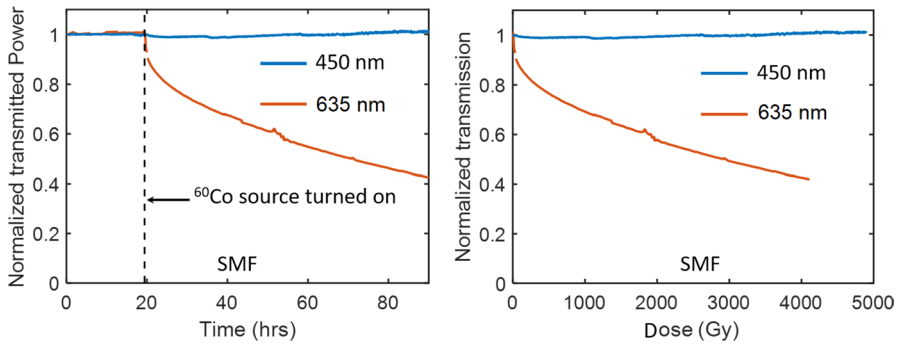

Fig. 6 Normalized transmitted optical power for MFG phosphors excitation/emission wavelengths through the Single mode fibre (SMF) as a function of time (left) and received dose (right)
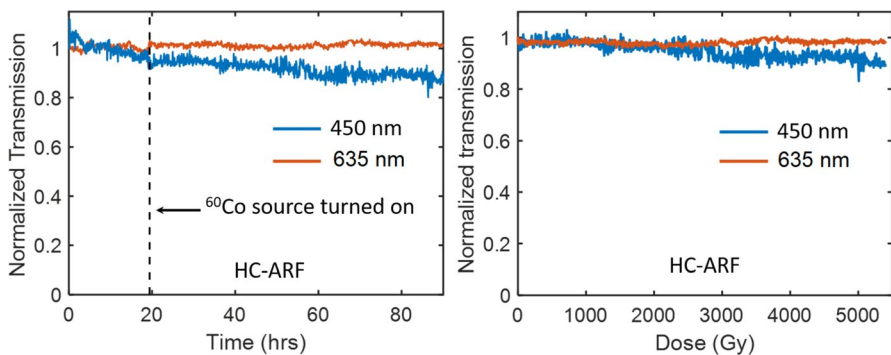

Fig. 7 Normalized transmitted optical power for MFG phosphors excitation/emission wavelengths through the hollow-core anti-resonant fibre (HCF) as a function of time (left) and received dose (right)

which manage to trap at perfect sites in the glass network. The work by Griscom et al. [23] confirms that gamma ray induced absorption band at 660 nm in pure and F-doped silica core fibres is due to self-trapped holes and Girard et al. [24] imply the latter to be the cause of radiation-induced absorption band in the blue domain.

Looking at the single mode fibres (Fig. 6), we see distinct behaviours at the blue and red wavelength. At 450 nm, virtually no change is observed in the transmission of the fibre up to the total 4.9 kGy it is exposed to. This is an equally surprising result. Although the manufacturer would not disclose any information regarding the glass composition, it specifies that this class of products is optimised to resist photodegradation in the visible domain, i.e., they are solarisation-resistant. We believe that the dopants added to improve this aspect of the fibre may also confer to it some radiation hard properties in the blue region.

At the red wavelength, the signal launched through the single mode fibre decays exponentially as it is exposed to the radiation, decreasing by 59 % in 72 h during which it absorbed approximately 4.1 kGy. This degradation of the transmission properties of the fibre is in line with expectations and together with the results of the radiation hard fibre, it goes to show the inherent difficulty faced by the common remedial techniques used to make an optical fibre resistant to ionising radiation. Indeed, dopants that may enhance the radiation hardness of the fibre in one spectral region may contribute to worsening it in another. Applications such as the one envisaged here would thus almost always require using different solid fibres for different wavelength bands. Whilst this is a possibility, we note that the transmission of red wavelengths in silica fibres is inherently more prone to degradation when exposed to radiation because the radiation-induced defects (colour centres) lead to photodarkening in this spectral region (cfr. Fig. 7 in [23]).

Finally, the transmission results through the HCF are shown in Fig. 7. Because of its position on the bobbin, the HCF sample received the highest dose of 5.4 kGy. We see immediately that at 635 nm, transmission through the fibre is virtually unaffected throughout the irradiation experiment. For the 450 nm signal, we see a slow decay throughout the experiment, with little change between the first 18 h without radiation and the subsequent 72 h where the radiation is on. This is due primarily to the fact that the 450 nm wavelength lies close to the edge of the anti-resonance window where transmission is more sensitive to small changes in the wavelength of the laser or small changes within the fibre. Indeed, were the laser wavelength to slowly drift over time, this would produce large changes in fibre attenuation because of this proximity to the window-edge. More plausibly however, given the 80 h timescale of the decay, the slow downward drift in transmission may be due to the pressure inside the fibre slowly equalising over time after the samples were spliced. Indeed, the attenuation of hollow-core fibres is sensitive to the gas pressure in the hollow regions which can change their refractive index [25]. Again, the 450 nm wavelength would be more sensitive to this due to its close proximity to the loss edge. Thus, we believe that a fibre with an improved design in which the blue laser wavelength lies near the centre of the anti-resonant window should, just like in the infrared in the current HCF, be immune to ionising radiation. In the meantime, these experimental results suggest that a radiation-resistant MFG-based fibre-optic thermometer can be
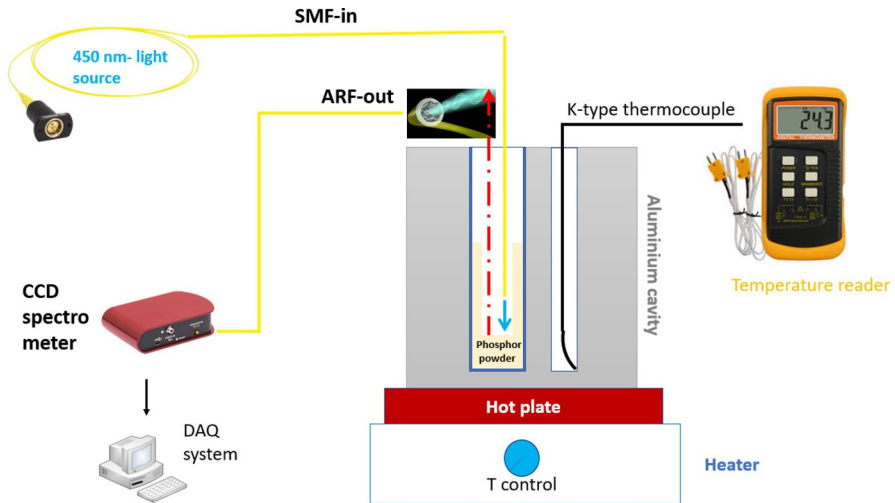
Fig. 8 Experimental set-up for temperature measurement based on MFG phosphorescence intensity ratio method
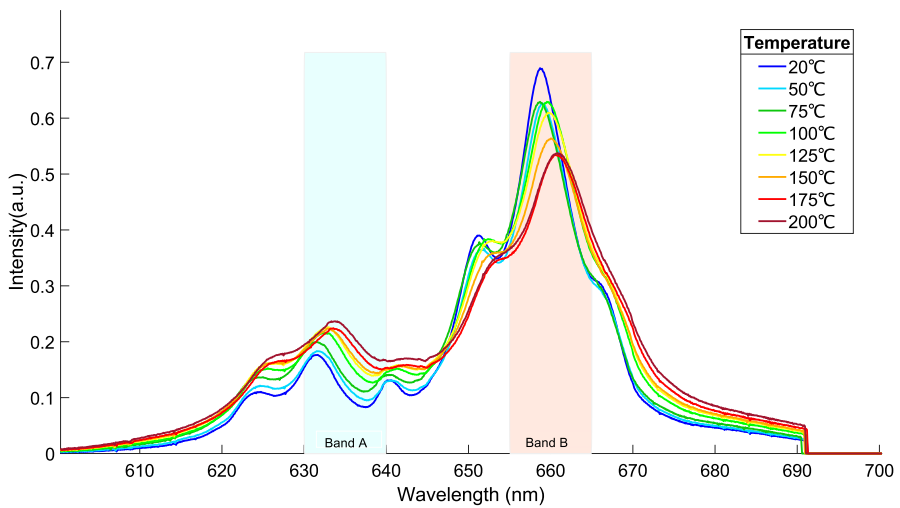

Fig. 9 MFG emission spectra at various temperatures with excitation at 450 nm

built by using the SMF to deliver the excitation light and using the HCF to collect the emitted signal from which the temperature can be monitored. We built such a thermometer and describe it in the following section.

6 HCF/SMF Phosphor Thermometer

With the results showing that a good combination for nuclear waste management phosphor thermometry would be solarisation resistant SMF for the blue excitation and AR-HCF for the red, we tested this combination using the set up shown in Fig. 8 based on the intensity ratio technique (cfr. Fig. 9). Though the amount of optical power generated by the excited phosphor would have been sufficient to implement the decay lifetime approach, we opted for the ratio method as the necessary equipment is less sophisticated. A few grams of powdered MFG phosphor was poured into a 4 cm-deep well drilled into an aluminium block. A K-type thermocouple was used for system calibration. The block was placed on a variable temperature hot plate. The phosphor was excited with a Thorlabs pigtailed 450 nm-laser diode connected to a 40 cm-long sample of the previously tested SMF with a cleaved end in direct contact with the MFG powder. In the same well, a 40 cm-long section of the previously tested HCF was placed in direct contact with the phosphor to collect the emitted red signal. Given the small numerical aperture of the HCF, the close proximity of the HCF sample to the phosphor ensured that the collection efficiency would be maximized. The spectrum of the signal coupled into the hollow fibre was measured with a Thorlabs CCS-100 CCD spectrometer.

The ratio of two bands (simulating bandpass filters 10 nm wide) was used to assess performance as a ratio thermometer. A second-order polynomial was fitted to each of three measurement cycles. Results are shown in Fig. 10 . The change from the first run in terms of temperature between cycles is shown in Fig. 11. Continuing changes at this level would be unacceptable in most practical applications. It turns out, however, that the higher temperatures to which both fibre samples are exposed in each run (> 150 °C) may have damaged their protective polymer coatings, thus altering their transmission properties. They can be replaced by alternative coating
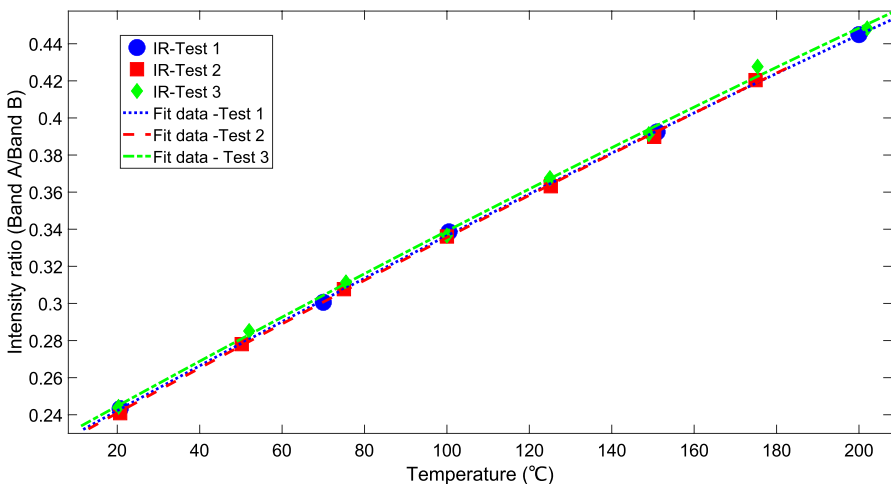

Fig. 10 Band A/Band B intensity ratios characterising three heating cycles plotted against temperatures measured with thermocouple
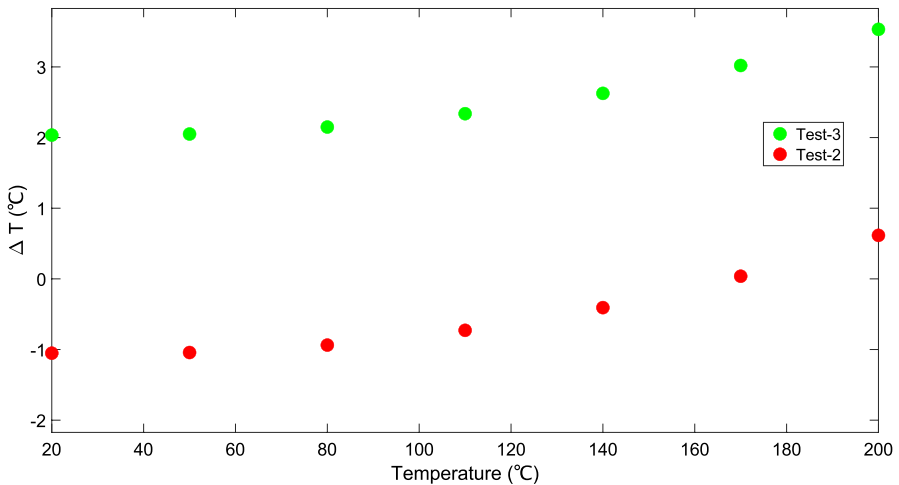
Fig. 11 Change in phosphor calibration characterising heating cycles 2 and 3 in comparison to cycle 1

materials which can withstand higher temperatures. We do, however, have a functioning thermometer, and the first ever that incorporates a novel hollow-core optical fibre.

7 Conclusions

We have shown that light guidance in a hollow or air-filled region endows novel hollow-core optical fibres with robust resistance to the effects of ionizing radiation. Our measurements of the power transmitted through a tubular anti-resonant fibre exposed to irradiation doses equivalent to 100 years in a nuclear waste storage environment unequivocally demonstrate this robustness at 635 nm. The slow downward drift in transmitted power over time at the 450 nm is not believed to be due to the fibre's response to irradiation, but rather to the fact the sample used here is not optimized for transmission at that wavelength. Such high resistance to ionizing radiation uniquely positions this novel class of optical fibres for applications in harsh environments, including the monitoring of temperature under extreme gamma radiation as explored in this work. We also found a commercial SMF sample to be surprisingly resistant to ionizing radiation at 450 nm, perhaps as an unintended consequence of it being designed to avoid damage from intense UV light. We therefore used this fibre in combination with the HCF to demonstrate, for the first time to the best of our knowledge, a functioning phosphor thermometer for use in ionizing radiation environments.

Also surprisingly, we consistently found that commercially available single mode fibres optimized for resistance to radiation in the infrared became rapidly opaque to visible wavelengths as soon as they were exposed to radiation, showcasing the challenges in engineering fibre materials to achieve radiation hardness across broad spectral regions.

An MFG fibre-optic thermometer for nuclear environments must exhibit significant immunity to ionising radiation at both the excitation and emission wavelengths of the phosphor, especially if the sensing scheme is based on spectral intensity changes. In this paper, a functioning prototype of such a device has been demonstrated over the range 20 °C to 200 °C. It incorporates the two different fibre samples that exhibited the highest resistance to radiation flux and fluence values typical of nuclear decommissioning, a commercial SMF sample for the excitation and, for the first time, a HCF sample to collect the red emission.

To realize the ultimate goal of building a radiation hard fibre thermometer employing only HCF samples, a few issues remain, notably tailoring the fibre design to simultaneously accommodate both the excitation and emission wavelengths of the MFG in the middle of their transmission bands. Unlike in solid-core fibres which would require changing the materials of the fibre, tuning the properties of the HCF to achieve this goal simply requires a careful control of the size and thicknesses of the tubes. Just as has been done to reduce their loss to levels comparable to or lower than those of solid-core fibres at other visible and infrared fibres, we believe the HCF structures will be optimized to meet the needs of phosphor thermometry in harsh environments.

Declarations

Conflict of interest The authors declare no conflict of interest.

References

1. *Decommissioning Nuclear Facilities: World Nuclear Association* (2021). https://www.world-nuclear.org/information-library/nuclear-fuel-cycle/nuclear-wastes/decommissioning-nuclear-facilities.aspx. Accessed July, 2021.
2. J.L. McMillan, A. Greenen, W. Bond, M. Hayes, R. Simpson, G. Sutton, G. Machin, J. Jowsey, A. Adamska, Thermometry of intermediate level waste containers using phosphor thermometry and thermal imaging. Measurement **132**, 207–212 (2019). https://doi.org/10.1016/j.measurement.2018.09.030

3. A. Sposito, E. Heaps, G. Sutton, G. Machin, R. Bernard, S. Clarke, Phosphor thermometry for nuclear decommissioning and waste storage. Nucl. Eng. Des. **375**, 111091 (2021). https://doi.org/10.1016/j.nucengdes.2021.111091

4. S. Girard, A. Morana, A. Ladaci, T. Robin, L. Mescia, J.-J. Bonnefois, M. Boutillier, J. Mekki, A. Paveau, B. Cadier, E. Marin, Y. Ouerdane, A. Boukenter, Recent advances in radiation hardened fiber-based technologies for space applications. J. Opt. **20**, 093001 (2018). https://doi.org/10.1088/2040-8986/aad271

5. H. Henschel, J. Kuhnhenn, U. Weinand, High radiation hardness of a hollow core photonic bandgap fiber, in *8th European Conference on Radiation and Its Effects on Components and Systems* (2005). https://doi.org/10.1109/RADECS.2005.4365659

6. F. Poletti, Nested antiresonant nodeless hollow core fiber. Opt. Express **22**, 23807–23828 (2014). https://doi.org/10.1364/OE.22.023807

7. H. Sakr, T.D. Bradley, G.T. Jasion, E. Numkam Fokoua, S.R. Sandoghchi, I.A. Davidson, A. Taranta, G. Guerra, W. Shere, Y. Chen, J.R. Hayes, D.J. Richardson, F. Poletti, Hollow core NANFs with five nested tubes and record low loss at 850, 1060, 1300 and 1625 nm. Opt. Fiber Commun. Conf. **2021**, 3–4 (2021). https://doi.org/10.1364/OFC.2021.F3A.4

8. G.T. Jasion, T.D. Bradley, K. Harrington, H. Sakr, Y. Chen, E.N. Fokoua, I.A. Davidson, A. Taranta, J.R. Hayes, D.J. Richardson, F. Poletti, Hollow core NANF with 0.28 db/km attenuation in the C and L bands, in *Optical Fiber Communication Conference Postdeadline Papers* (2020). https://doi.org/10.1364/OFC.2020.Th4B.4

9. H. Sakr, Y. Chen, G..T. Jasion, T..D. Bradley, J..R. Hayes, H..C..H. Mulvad, I..A. Davidson, E. Numkam Fokoua, F. Poletti, Hollow core optical fibres with comparable attenuation to silica fibres between 600 and 1100 nm. Nat. Commun. **11**, 1–10 (2020). https://doi.org/10.1038/s41467-020-19910-7

10. S.-F. Gao, Y.-Y. Wang, W. Ding, Y. Hong, P. Wang, Conquering the Rayleigh scattering limit of silica glass fiber at visible wavelengths with a hollow-core fiber approach. Laser Photonics Rev. **14**, 1–6 (2020). https://doi.org/10.1002/lpor.201900241

11. F. Poletti, M.N. Petrovich, D.J. Richardson, Hollow-core photonic bandgap fibers: technology and applications. Nanophotonics **2**, 315–340 (2013). https://doi.org/10.1515/nanoph-2013-0042

12. C. Wei, R. Joseph Weiblen, C.R. Menyuk, J. Hu, Negative curvature fibers. Adv. Opt. Photonics **9**, 562 (2017). https://doi.org/10.1364/aop.9.000562

13. N.M. Litchinitser, A.K. Abeeluck, C. Headley, B.J. Eggleton, Antiresonant reflecting photonic crystal optical waveguides. Opt. Lett. **27**, 1592–1594 (2002). https://doi.org/10.1364/OL.27.001592

14. F. Yu, J.C. Knight, Negative curvature hollow-core optical fiber. IEEE J. Sel. Top. Quantum Electron. **22**, 146–155 (2016). https://doi.org/10.1109/JSTQE.2015.2473140

15. G.T. Jasion, T.D. Bradley, K. Harrington, H. Sakr, Y. Chen, E. Numkam Fokoua, I.A. Davidson, A. Taranta, J.R. Hayes, D.J. Richardson, F. Poletti, Recent breakthroughs in hollow core fiber technology, in *Optical Fiber Communications Conference* (2021). https://doi.org/10.1364/OFC.2021.M5E.2, http://www.osapublishing.org/abstract.cfm?URI=OFC-2021-M5E.2. Accessed November, 2021.

16. H. Henschel, Radiation hardness of present optical fibres, in *Proceeding SPIE 2425, Optical Fibre Sensing and Systems in Nuclear Environments* (1994). https://doi.org/10.1117/12.198638

17. S.W. Allison, G.T. Gillies, Remote thermometry with thermographic phosphors: instrumentation and applications. Rev. Sci. Instrum. **68**, 2615–2650 (1997). https://doi.org/10.1063/1.1148174

18. C. Abram, B. Fond, F. Beyrau, Temperature measurement techniques for gas and liquid flows using thermographic phosphor tracer particles. Prog. Energy Combust. Sci. **64**, 93–156 (2018). https://doi.org/10.1016/j.pecs.2017.09.001

19. A.H. Khalid, K. Kontis, Thermographic phosphors for high temperature measurements: principles, current state of the art and recent applications. Sensors **8**, 5673–5744 (2008). https://doi.org/10.3390/s8095673

20. A. Ali, L.S. Khanzada, A. Hashemi, C. Polzer, A. Osvet, C. Brabec, M. Batentschuk, Optimization of synthesis and compositional parameters of magnesium germanate and fluoro-germanate thermographic phosphors. J. Alloy. Compd. **734**, 29–35 (2018). https://doi.org/10.1016/j.jallcom.2017.10.259

21. B. Brichard, A.L. Tomashuk, V.A. Bogatyrjov, A.F. Fernandez, S.N. Klyamkin, S. Girard, F. Berghmans, Reduction of the radiation-induced absorption in hydrogenated pure silica core

fibres irradiated in situ with γ-rays. J. Non-Cryst. Solids **353**, 466–472 (2007). https://doi.org/10.1016/j.jnoncrysol.2006.10.039

22. G. Machin, R. Simpson, G. Sutton, W. Bond, E. Heaps, M. Hayes, S. Korniliou, J. McMillan, J. Norman, A. Sposito, V. Panicker, A. Adamska, A. Allen, R. Bernard, S. Clarke, J. Clifford, C. Gallagher, J. Jowsey, Novel thermometry approaches to facilitate safe and effective monitoring of nuclear material containers. Nucl. Eng. Des. **371**, 110939 (2021). https://doi.org/10.1016/j.nucengdes.2020.110939

23. D. Griscom, γ-ray-induced visible/infrared optical absorption bands in pure and f-doped silica-core fibers: are they due to self-trapped holes? J. Non-Cryst. Solids **349**, 139–147 (2004). https://doi.org/10.1016/j.jnoncrysol.2004.08.221

24. S. Girard, J. Kuhnhenn, A. Gusarov, B. Brichard, M. Van Uffelen, Y. Ouerdane, A. Boukenter, C. Marcandella, Radiation effects on silica-based optical fibers: recent advances and future challenges. IEEE Trans. Nucl. Sci. **60**, 2015–2036 (2013). https://doi.org/10.1109/TNS.2012.2235464

25. T.W. Kelly, P. Horak, I.A. Davidson, M. Partridge, G.T. Jasion, S. Rikimi, A. Taranta, D.J. Richardson, F. Poletti, N.V. Wheeler, Gas-induced differential refractive index enhanced guidance in hollow-core optical fibers. Optica **8**, 916–920 (2021). https://doi.org/10.1364/OPTICA.424224

Publisher's Note Springer Nature remains neutral with regard to jurisdictional claims in published maps and institutional affiliations.

Authors and Affiliations

Nicolò Pisani[1] ⓘ **· Eric Numkam Fokoua[1] · Ian A. K. Davidson[1] · Francesco Poletti[1] · Radan Slavík[1] · Dave Lowe[2] · Graham Machin[2] · Gavin Sutton[2]**

Eric Numkam Fokoua
Eric.Numkam-Fokoua@soton.ac.uk

Ian A. K. Davidson
I.A.K.Davidson@soton.ac.uk

Francesco Poletti
frap@soton.ac.uk

Radan Slavík
R.Slavik@soton.ac.uk

Dave Lowe
dave.lowe@npl.co.uk

Graham Machin
graham.machin@npl.co.uk

Gavin Sutton
gavin.sutton@npl.co.uk

[1] Optoelectronic Research Centre (ORC), University of Southampton, University Road, Southampton, Hampshire SO17 1SJ, UK

[2] Department of Thermal and Radiometric Metrology, National Physical Laboratory, Queens Road, Teddington, Middlesex TW11 0LW, UK